Proceedings of the Second International Conference on Press-in Engineering 2021, Kochi, Japan – Matsumoto et al (eds)

Influence of different pile installation methods on vertical and horizontal resistances

S. Moriyasu
Nippon Steel Corporation, Tokyo, Japan

M. Ikeda
Kanazawa City Government, Kanazawa, Japan (former student of Kanazawa University)

T. Matsumoto, S. Kobayashi & S. Shimono
Kanazawa University, Kanazawa, Japan

ABSTRACT: This study focuses on the influence of the pile installation method on vertical and horizontal pile resistance. In a series of laboratory experiments, a model pile was installed using four types of pile installation methods: monotonic push-in, surging (repetitive push-in and pull-out), vibratory pile driving, and bored pile installation in dense dry sand ground. It was found that the cyclic shearing of surging or vibratory pile driving prevented soil dilation and decreased pile penetration resistance. During a static load test in the vertical direction, the pile installed using push-in, surging, or vibratory pile driving exhibited a higher vertical resistance in comparison with the bored pile installed in a similar manner. In the horizontal load tests, relatively high horizontal resistances were obtained in the surging and push-in cases in comparison with the bored pile, indicating that the effect of the displacement pile increases the horizontal soil resistance.

1 INTRODUCTION

In Japan, owing to the occurrence of many earthquakes, the assessment of the horizontal and vertical resistances (i.e., bearing capacity) of a pile is important. Although many types of pile installation methods exist, the difference in the horizontal resistance of a pile installed by each piling method has not been fully clarified yet. Therefore, this study investigates the influence of different piling methods on the horizontal pile resistance, and correlation between the horizontal resistance and the vertical resistance.

It is well known that the vertical resistance depends on the pile installation method. Some studies (e.g., Jack-in installation method: White & Deeks 2007, Ogawa et al. 2011; Vibratory pile driving: Holeyman et al. 1996, Vanden Berghe 2001) have

clarified that pile movement during pile penetration causes soil dilation or contraction. Moriyasu et al. (2020) investigated the influence of the pile installation method on the vertical resistance of a model pile in sand ground through a series of laboratory experiments. It was discovered that while the pile installation force in surging or vibratory pile driving was lower than that in monotonic push-in, the bearing capacity of the pile installed in these methods was the same or higher than that in the monotonic push-in. According to Moriyasu et al. (2020), soil contraction caused by cyclic pile movement during pile installation transforms into soil dilation under monotonic shearing during the static load test. However, Moriyasu et al. (2020) treated only the displacement pile installation methods. Therefore, this study adopted the bored pile method as a representative non-displacement pile installation method and compared the vertical resistance with those of the displacement pile installation methods. In a series of laboratory experiments, a model pile was installed using four different piling methods, i.e., push-in, surging, vibratory pile driving and boring (buried). After the pile installation process, vertical load test (VLT) and horizontal load test (HLT) were conducted.

2 EXPERIMENTAL DESCRIPTION

2.1 *Experimental cases*

Table 1 presents the experimental cases and conditions. Each experiment comprised a pile penetration test (PPT), VLT, and HLT. In Case 1, a model pile was installed using a monotonic push-in at a penetration

DOI: 10.1201/9781003215226-21

Table 1. Experimental cases and conditions.

Case No.	Case 1	Case 2	Case 3	Case 4
Relative density, D_r (%)	80	80	80	80
Penetration method	push-in	surging	vibration	bored pile
Penetration rate (mm/s)	0.15	0.15	-	-
Vibration frequency (Hz)	-	-	25 ~ 55	-
Test sequence	PPT*1 ↓ VLT*2 ↓ HLT*3 ↓ CPT*4	PPT ↓ VLT ↓ HLT ↓ CPT	Static loading by V.H. *5 weight ↓ Vibration ↓ VLT ↓ HLT ↓ CPT	Embedded with ground preparation ↓ VLT ↓ HLT ↓ CPT

* 1 PPT: pile penetration test, *2 VLT: vertical load test, *3 HLT: horizontal load test, *4 CPT: cone penetration test, *5 V.H.: vibratory hammer.

rate of 0.15 mm/s during a PPT. In Case 2, surging implies the repetition of 4 mm push-in (downward) and 2 mm pull-out (upward) strokes. In Case 3, a vibratory hammer model was employed to install a model pile. In Case 4, a model pile was embedded in the ground during model ground preparation. After the PPT, both the VLT and HLT were performed continuously.

2.2 *Model pile*

A closed-ended aluminium pipe pile with a diameter of 32 mm, wall thickness of 1.3 mm, and length of 600 mm was used for the model pile. As shown in Figure 1, two strain gauges were attached on opposite faces at each level to calculate the axial strains and bending strains. The pile surface with the strain gauges was coated with an acrylic adhesive and glued with silica sand, i.e., the same material used for the model ground.

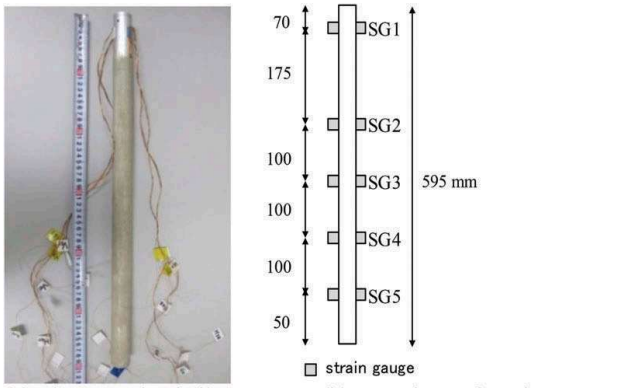

(a) Photograph of pile (b) Locations of strain gauges

Figure 1. Model pile.

2.3 *Model ground*

Silica sand was used as the model ground material in all cases. Table 2 lists the physical properties of the sand. The model ground was prepared in a cylindrical soil container of diameter 566 mm and height 580 mm. The silica sand was poured into a container divided into 12 model ground layers (11 layers of height 50 mm and one layer of height 30 mm). The sand was compacted using a small tamper to adjust the relative density D_r to 80 %. The reason for choosing such a high relative density is to investigate the pile behaviour in a dense sand condition and obtain the soil resistance against the pile clearly within a short penetration depth.

2.4 *Experimental apparatus and procedure*

During the PPT, the model pile was installed into the model ground until the pile head displacement w_h reached approximately 420 mm by push-in, surging, and vibration. In the cases of push-in and surging, an electrical jack, shown in Figure 2(a), was employed. While the pile was installed monotonically at a pile penetration rate of 0.15 mm/s in the push-in case, it was installed with the repetitions of 4 mm push-in and 2 mm pull-out strokes at a pile movement speed of 0.15 mm/s in the surging case. The pile head load, P_h, was measured using a load cell between the pile head and jack. Figure 2(b) shows the vibratory hammer model employed in the vibration case. The vibratory hammer model weighed 275 N and had a maximum frequency of 60 Hz.

Vibration was generated by two electric motors with an eccentric mass, as shown in Figure 2(b). When the motors were rotated in opposite directions, the horizontal vibrations were negated, and the vertical vibrations of the two motors were harmonised. At the beginning of the PPT in the vibration case, the pile was installed by the weight of the vibratory hammer alone. When it became difficult to install the pile by the self-weight of the hammer, the vibration began. Until w_h reached approximately 420 mm, if the pile penetration stopped, the vibration frequency was

Table 2. Physical properties of silica sand.

Minimum dry density, ρ_{dmin}	(t/m^3)	1.37
Maximum dry density, ρ_{dmax}	(t/m^3)	1.63
Maximum void ratio, e_{max}		0.96
Minimum void ratio, e_{min}		0.65
Mean particle size, D_{50}	(mm)	0.51

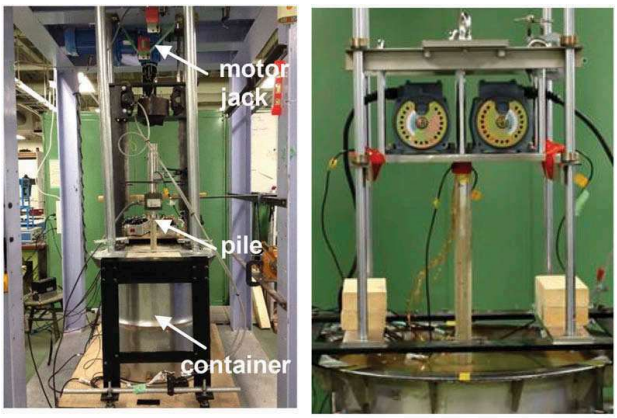

(a) Motor jack (b) Vibratory hammer model

Figure 2. Loading apparatus for pile penetration test and vertical load test.

increased to enhance the pile installation. The P_h was estimated from the strains near the pile top (i.e., SG1).

Subsequently, a VLT was performed. In all cases, the pile head was pushed by the electrical jack at a rate of 0.1 mm/s until w_h reached 440 mm. In the case of bored (buried) piles, the pile was embedded at a depth of 420 mm during the preparation stage of the model ground. During the VLT, the bored pile was pushed from a depth of 420 to 440 mm. In all cases, P_h was measured using the load cell between the pile head and jack.

After the VLT, an HLT was conducted. As shown in Figures 3 and 4, the pile head was pulled using a wire and a hand winch. An accelerometer was employed to obtain the slope-deflection at the pile top. The relationship between the inclined angle and acceleration was calibrated in advance.

Finally, cone penetration tests (CPTs) were performed to investigate the ground condition after the piling tests. A rod with a circular cone with a diameter of 20.05 mm at the tip was jacked at four locations in the model ground using an electrical jack (see Figure 4). After the CPT, the pile was removed.

2.5 *Monotonic and cyclic triaxial shear tests of sand*

Consolidated monotonic and cyclic shear tests were performed to investigate the mechanical properties of the sand. The confining pressure of the tests was approximately 100 kPa. Figure 6 shows the results of the triaxial consolidated drained shear tests (CD tests) of dense sand (D_r = 82%). For the result of the monotonic loading case, Figure 6(a) shows the softening behaviour after the axial strain, ε_a, exceeds 5%. The internal friction angle at the peak strength,

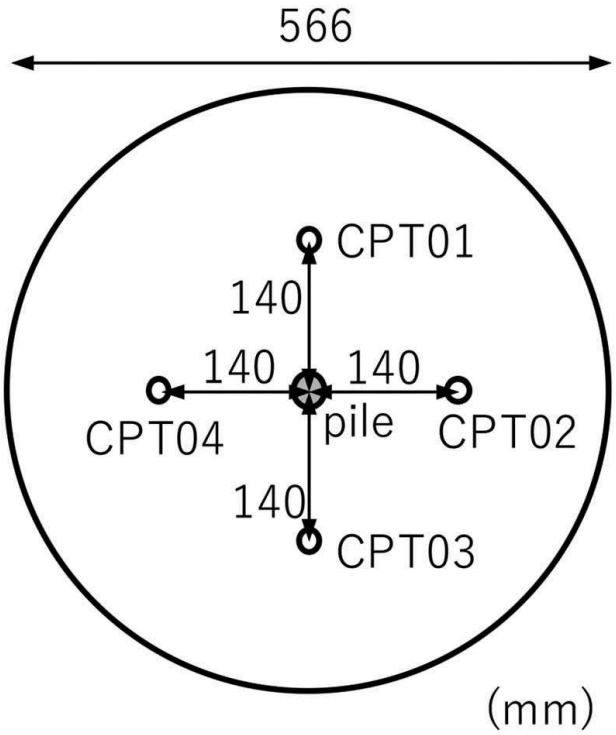

Figure 4. Locations of cone penetration tests.

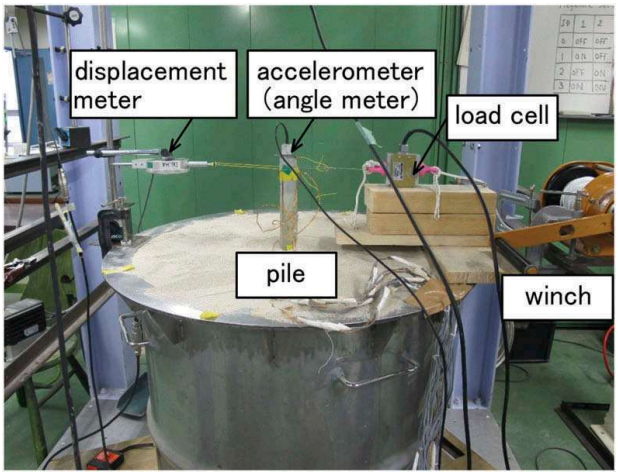

Figure 3. Loading apparatus for horizontal load test.

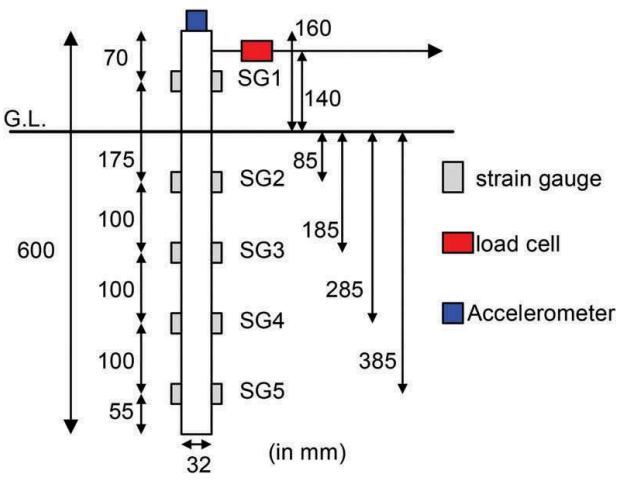

Figure 5. Schematic diagram of horizontal load test.

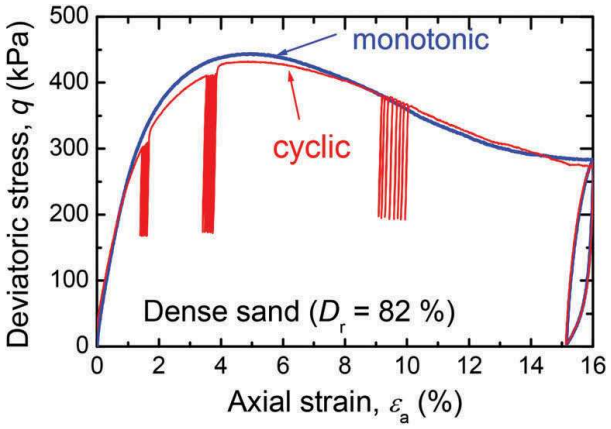

(a) Axial strain ε_a vs. deviatoric stress q

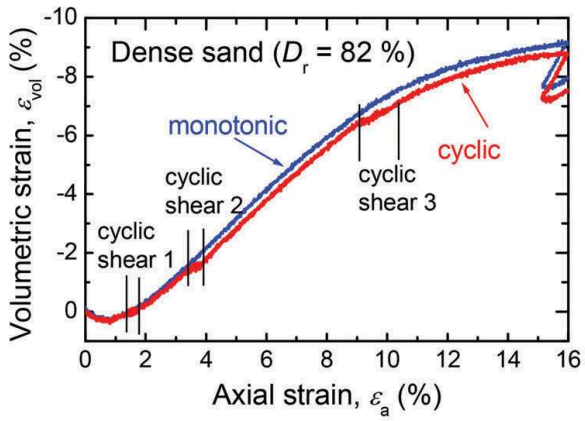

(b) Axial strain ε_a vs. volumetric strain ε_{vol}

Figure 6. Results of triaxial CD tests in dense ground.

ϕ_p', was 42.8° and that at the residual state, ϕ_r', was approximately 35.0°. In the case of cyclic loading, cyclic shearing was applied when ε_a reached 1.3%, 3.4%, and 8.9%, separately, by changing the axial stress, σ_a, with a constant radial stress, σ_r, of 100 kPa. According to the volumetric strain in Figure 6 (b), the volume increase during the cyclic shearing stages was smaller than that of the monotonic shearing case. This indicates that cyclic shearing prevented soil dilation. When the cyclic shearing transformed to monotonic shearing, the q–ε_a and ε_a–ε_{vol} relationships were similar to the corresponding curves of the monotonic shearing case.

3 RESULTS

3.1 *Results of cone penetration tests*

Figure 7 shows the distributions of the CPT tip resistance, q_t, with depth, z, for all cases. Each line represents the average of q_t at four CPT locations for each case. As shown in Figure 7, the q_t of Case 4 (bored pile) was smaller than those of other cases. Because the q_t in Cases 1, 2, and 3 (push-in, surging, and vibration, respectively) was higher than that in

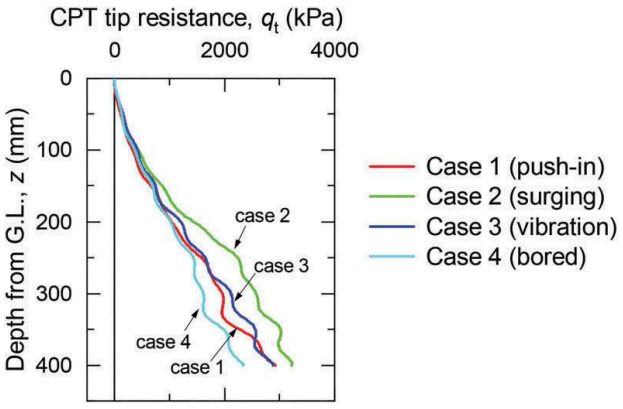

Figure 7. Results of cone penetration tests.

Case 4 (bored pile), the pile installation in Cases 1, 2, and 3 (displacement pile cases) would have increased the strength of soil around the pile.

3.2 *Results of pile penetration tests and vertical load tests*

Figure 8 shows the relationship between P_h and w_h for Cases 1, 2, and 3. At the end of the PPT (w_h = 420 mm), the P_h in Case 2 (surging) was smaller than that in Case 1 (push-in). Furthermore, the P_h in Case 3 (vibration) was much smaller than those in Cases 1 and 2. As mentioned above, cyclic CD tests show that cyclic shearing prevented soil dilation. If a similar behaviour of the soil occurred in Cases 2 and 3, the cyclic pile movement by surging or vibration would generate soil contraction around the pile. Because the cycle number, n, of the pile vibration in Case 3 was much higher than that in Case 2 (Case 2: n = 210, Case 3: $n \approx$ 21,600), the effect of cyclic shearing may be significant in Case 3.

For the result of the VLT, Figure 9 shows the relationship among the w_h, P_h, pile base resistance, P_b, and pile shaft resistance, P_s. P_b is the axial force obtained from strain gauge SG5, whereas P_s is the difference between P_h and P_b. As shown in Figure 9(a), the P_h, in the cases of displacement pile (Cases 1, 2, and 3) was higher than that in Case 4 (bored pile). Figure 9(b) shows that P_b and its stiffness in Cases 1, 2, and 3 were much higher than those in Case 4. Meanwhile, as shown in Figure 9(c), P_s and its stiffness in Cases 1 and 2 were similar to those in Case 4. Regarding the vibration (Case 3), after P_s reached a peak value, it decreased significantly. Figure 10 shows the distribution of increment of unit shaft resistance, $\Delta\tau_s$, during VLT.$\Delta\tau_s$ equals zero at the beginning of VLT, and each line shows the increment of unit shaft resistance when P_s reaches each number illustrated in Figure 9(c). When P_s decreased significantly (#1 to #2), Figure 10 shows that $\Delta\tau_s$ from ground surface to z = 78 mm and $\Delta\tau_s$ from z = 278 mm to z = 378 mm decreased largely.

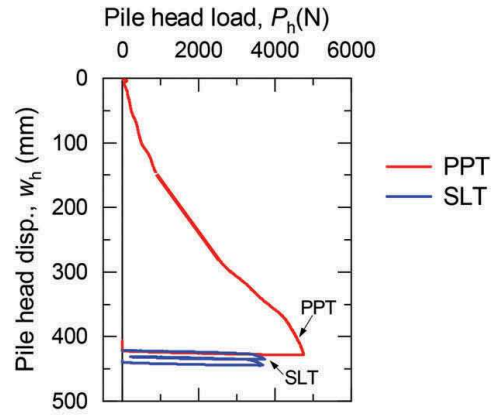

(a) Case 1 (push-in)

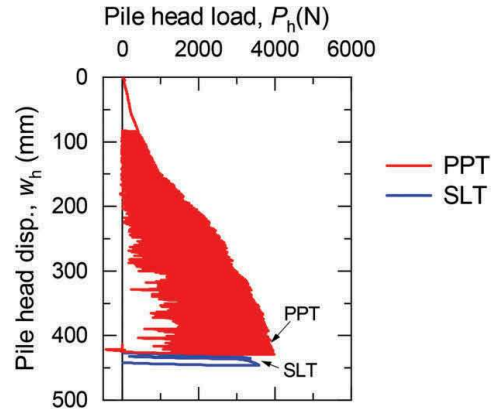

(b) Case 2 (surging)

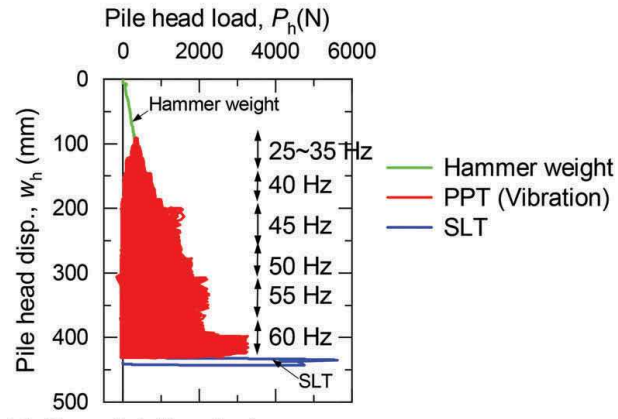

(c) Case 3 (vibration)

Figure 8. Relationship between pile head load, P_h, and pile head displacement, w_h, during PPT and VLT.

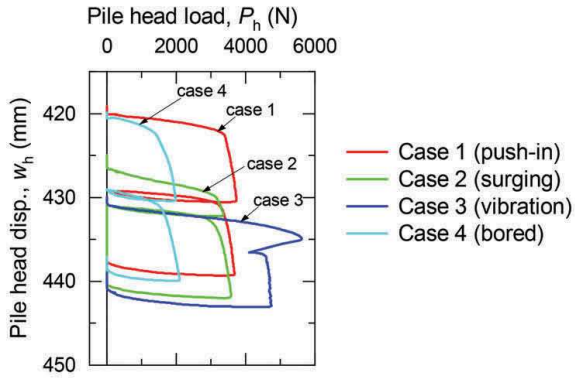

(a) Relationship between pile head load, P_h, and pile head displacement, w_h, during VLT.

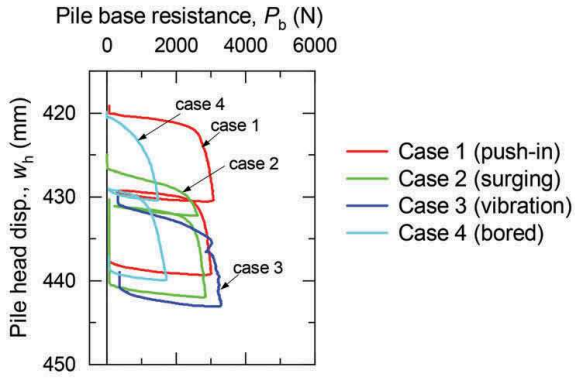

(b) Relationship between pile base resistance, P_b, and pile head displacement, w_h, during VLT.

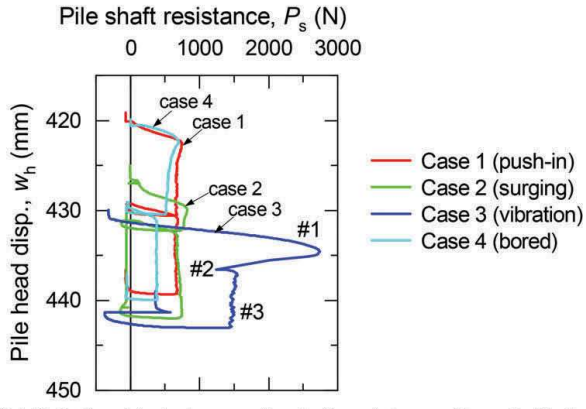

(c) Relationship between pile shaft resistance, P_s, and pile head

Figure 9. Results of vertical load test.

A possible reason why P_s decreased suddenly is that a hardening zone around the pile shaft formed during the PPT is sheared within a certain pile displacement during SLT. This hypothesis is based on a previous study which investigated a pile shaft resistance under a large number of quasi-static cyclic pile movements in a sand model ground (Bekki et al. 2013). As a result of the study, after the pile shaft friction was degraded by 300 cycles of pile movement, the friction kept increasing until the end of test (10^5 cycles). Bekki et al. (2013) pointed out that a large number of cycles progresses a densification of the sand within the interface zone around the pile. If a similar phenomenon occurred in the vibration case (Case 3), a large number of cyclic pile movement turns the aforementioned soil contraction to forming a hardening zone around the pile shaft. As a result, the P_h during PPT may increase gradually (see Figure 8 (c)). At the beginning of SLT, the hardening zone could increase P_s and its stiffness. When a certain monotonic pile displacement during SLT sheared the hardening zone, P_s decreased suddenly. Although such a softening occurred, as shown in

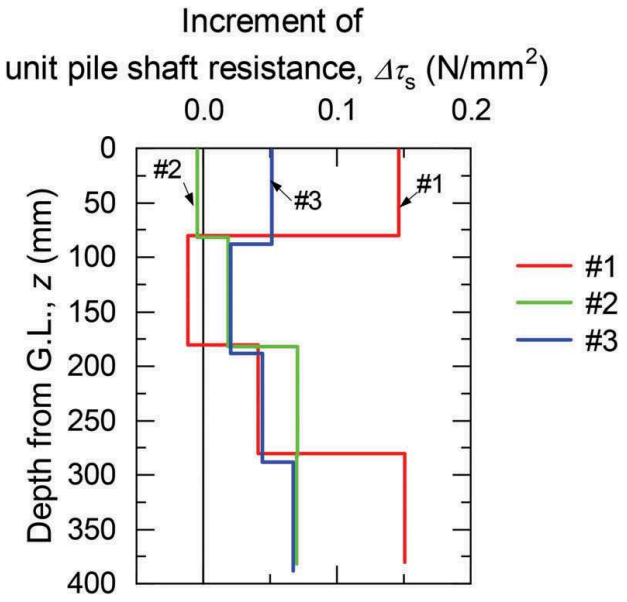

Figure 10. Increment of unit pile shaft resistance, $\Delta\tau_s$, during VLT in Case 3 (vibration).

Figure 9, the P_s and P_h in the vibration remained higher than those in other cases.

While the P_h in Cases 2 and 3 (surging and vibration) during the PPT was smaller than that in Case 1 (push-in), the VLT indicated that the P_h in Cases 2 and 3 was the same or higher than that in Case 1. From the results of the cyclic triaxial CD test, it was presumed that the monotonic shearing phase after cyclic shearing enhanced soil dilation. When the cyclic pile movement during the PPT transformed into monotonic movement during the VLT, soil dilation occurred.

Returning to Figure 8, P_h during the VLT is lower than those during the PPT in Cases 1 and 2. A possible reason is the difference of the pile penetration rate between PPT and VLT. Watanabe and Kusakabe (2013) found that the failure strength of sand increases with increasing the loading rate. Because the pile penetration rate during VLT (0.1 mm/s) was slower than that during PPT (0.15 mm/s), P_h during the VLT was lower than those during the PPT.

3.3 *Results of horizontal load tests*

Figure 11 shows the relationship between the horizontal load, H, and horizontal displacement at the loading level, u. H was measured using a load cell connected between the pile head and the winch. As shown in Figure 11, whereas the H in Cases 1 and 2 (push-in and surging) was higher than that in Case 4 (bored pile), the H in Case 3 (vibration) was similar to that in Case 4.

Figure 12 presents the influence of the pile installation method on the pile head load during the VLT or HLT. In Figure 12, the horizontal axis represents the ratio of the pile head load in displacement pile cases

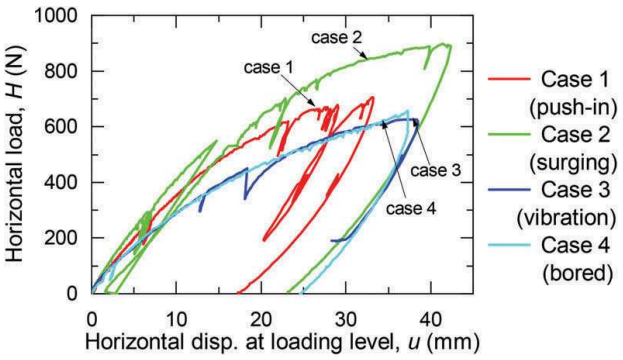

Figure 11. Relationship between pile head load, H, and horizontal displacement at loading level, u, during HLT.

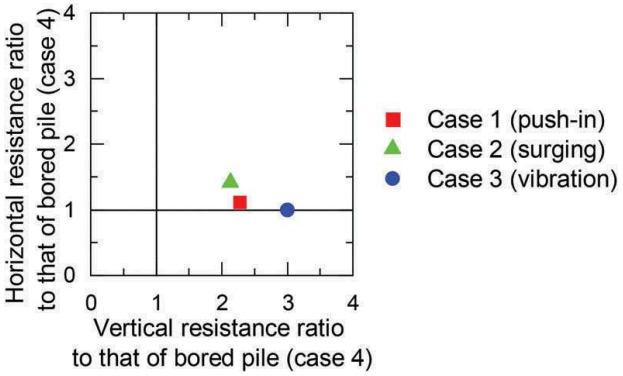

Figure 12. Pile resistance ratio of displacement pile cases to bored pile case in both VLT and HLT.

(Cases 1, 2, and 3) to Case 4 (bored pile) during the VLT, and the vertical axis indicates the same ratio during the HLT. To estimate the ratio of the VLT, the yield load in each case was employed. Because the softening of the pile head load was observed in Case 3 (see Figure 9(a)), the converged value after the softening (4,200 N) was selected. Regarding the ratio in the HLT, when the horizontal displacement at the loading level, u, was 30 mm, the horizontal load was employed in each case. While the ratio in the VLT ranged from 2.1 to 3.0, that in the HLT ranged from 1.0 to 1.4. Therefore, as shown in Figure 12, the influence of the pile installation method on H was less prominent in comparison with that on the vertical load, P_h, in the VLT.

Figures 13(a)-(c) show the horizontal pile behaviours at representative horizontal displacements, u, in Case 1. Figure 13(a) shows the bending moment distribution of the pile, which was obtained from the pile's flexural stiffness and measured bending strains. Figure 13(b) shows the distributions of lateral displacements of the pile, which were calculated from the second-order integration of the bending moment distribution, pile head horizontal displacement, and slope-deflection at the pile head. Figure 13(c) shows the horizontal soil pressure, p, acting on the pile shaft at representative depths of z = 85 and 385 mm.

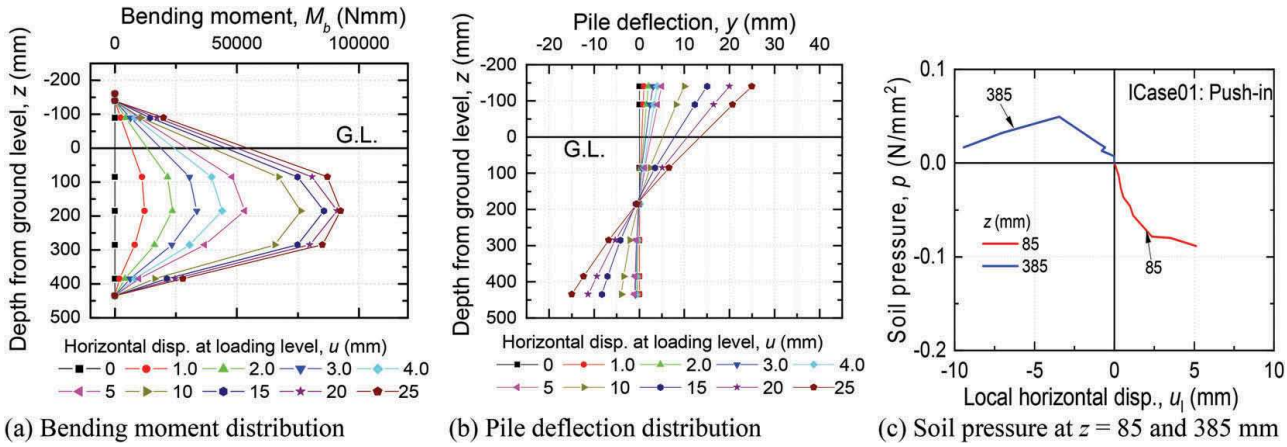

(a) Bending moment distribution (b) Pile deflection distribution (c) Soil pressure at z = 85 and 385 mm

Figure 13. Results of horizontal load test: Case 1 (push-in).

The soil pressure, p, was estimated from the second-order differential of the bending moment, M_b, and all p was the compressive stress. If the depth is shallower than the pile rotation centre, then the horizontal local pile displacement increases in the positive (plus) direction, and p exerts in the negative (minus) direction. Meanwhile, if the depth is greater than the rotation centre, then the local pile displacement increases in the negative (minus) direction, and p exerts in the positive (plus) direction. Figures 14 to 16 show the same pile behaviours for Cases 2 to 4.

The bending moment distributions ((a) in Figures 13 to 16) show that the M_b in Cases 1 and 2 was larger than that in Cases 3 and 4 at the same u. This order of M_b corresponds to the order of H, as shown in Figure 11.

As shown in (b) of Figures 13 to 16, the pile rotated with increasing u. While the centre of the pile rotation was at approximately z = 200 mm (z = depth from the ground level) in Cases 1, 2, and 4, that in Case 3 was at z = 300 mm. The deeper centre of the pile rotation in Case 3 indicates that the horizontal earth pressure on the pile was lower than those in the other cases. Here, the pile deflection distribution in Case 3 was not obtained after u = 10 mm because the accelerometer for measuring the pile head slope-deflection was not available owing to technical reasons.

While the pile shaft resistance in Case 3 (vibration) during VLT was higher than those in other cases, the horizontal soil pressure, p, during HLT was not higher than other cases. From this result, the soil condition in the vibration case is presumed as shown in Figure 17. As mentioned above, a large number of vibration during PPT may form a hardening zone surrounding the pile and increase the pile shaft resistance in the vertical direction (i.e., in VLT). Because the hardening associates with densification, the soil in the outer zone is loosened when the pile is vertically loaded statically after the installation. Therefore, when the pile is loaded in the horizontal direction (i.e., HLT), the outer loosened zone could have small horizontal pile resistance. More investigations are required to clarify this hypothesis.

In addition, in Case 2 (surging), whereas the pile penetration resistance during the PPT was smaller than that in Case 1 (push-in), the VLT and HLT demonstrated the same or higher resistances than that in

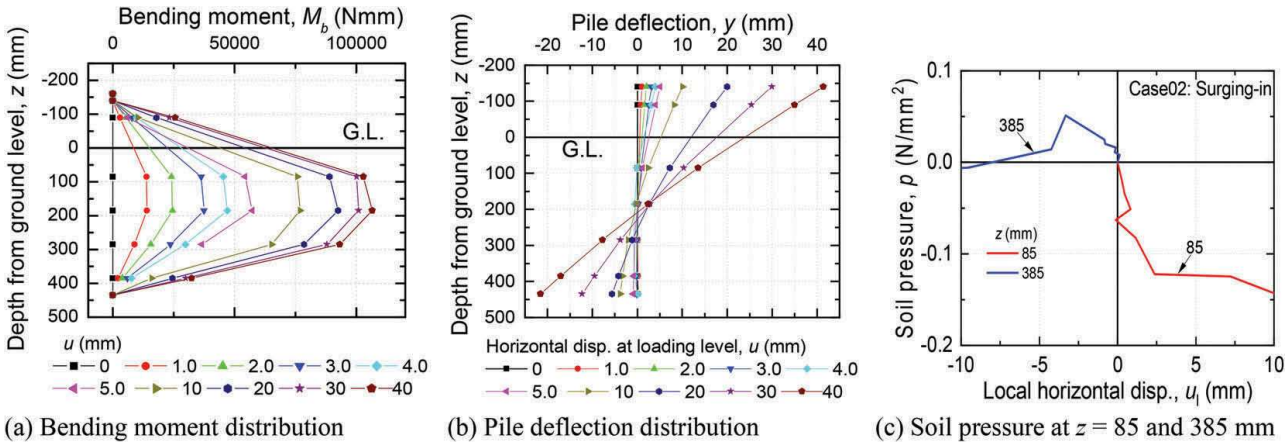

(a) Bending moment distribution (b) Pile deflection distribution (c) Soil pressure at z = 85 and 385 mm

Figure 14. Results of horizontal load test: Case 2 (surging).

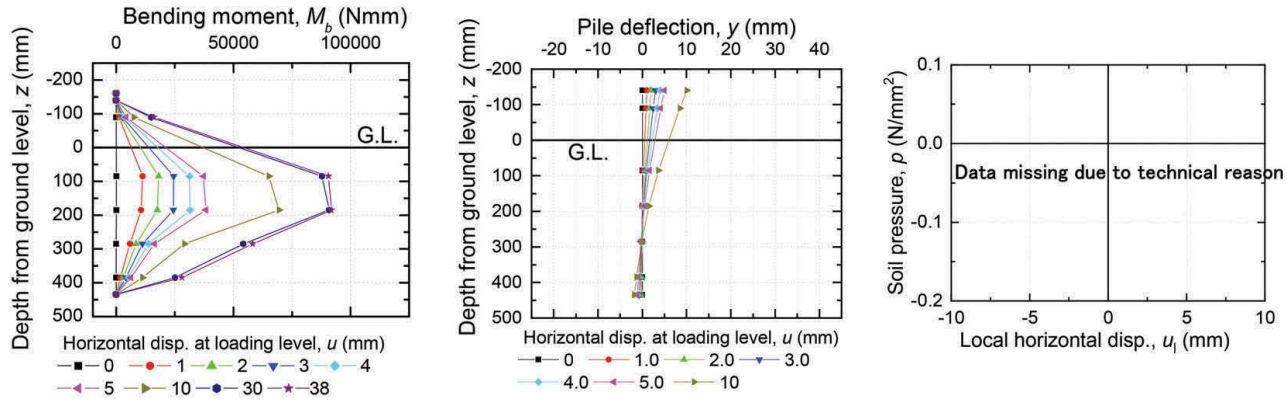

(a) Bending moment distribution (b) Pile deflection distribution (c) Soil pressure at z = 85 and 385 mm

Figure 15. Results of horizontal load test: Case 3 (vibration).

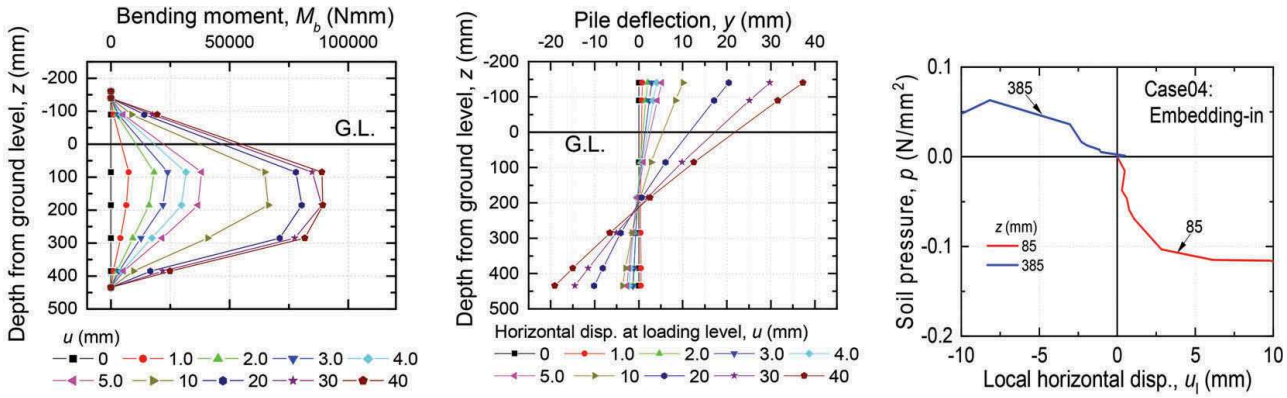

(a) Bending moment distribution (b) Pile deflection distribution (c) Soil pressure at z = 85 and 385 mm

Figure 16. Results of horizontal load test: Case 4 (bored pile).

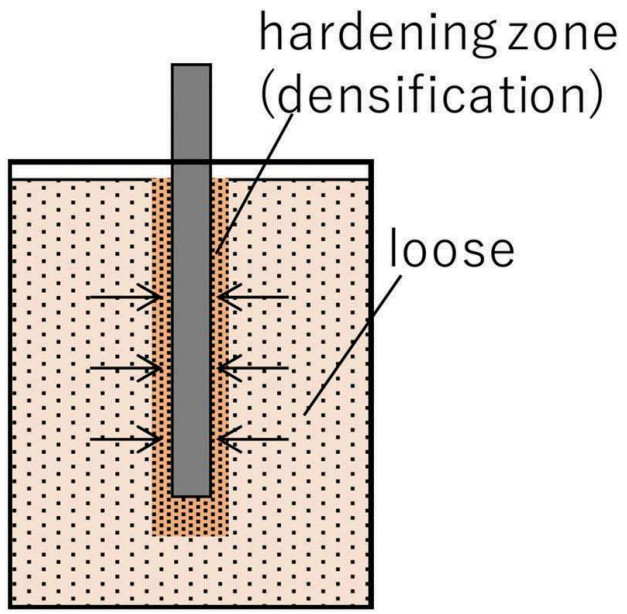

Figure 17. A concept of the soil condition in Case 3 (vibration).

Case 1. Settlements of the ground surface just after the end of installation in each test were not measured in the experiments. However, relative large settlement (2 to 4 mm by visual inspection) occurred at the ground surface within 2 or 3 mm from the pile shaft. Currently, the mechanism that yielded these results has not been clarified. Further studies are required to understand the relationship between the pile installation methods and the vertical or horizontal resistance.

Among (c) of Figures 13 to 16, p at the location of SG2 (z = 85 mm) in Case 2 was the highest at a specified local pile displacement, u_l, (i.e., the local pile displacement attached strain gauge SG2 in this case). This corresponded to the highest horizontal resistance shown in Figure 11. Meanwhile, the p at SG5 (z = 385 mm) was similar in all cases. Furthermore, as shown in (c) of Figures 13 to 16 that almost all of p–u_l relations showed a yield stress at a local pile displacement of approximately 2.0 mm, corresponding to u = 10 mm. It was presumed that the soil stress reached the yield stress, and that the residual stress state occurred by a local pile displacement of 2.0 mm.

4 CONCLUSIONS

The influence of different pile installation methods on the vertical and horizontal pile resistance were investigated in a series of laboratory experiments using a dense dry model ground. The major findings were as follows:

1) While the P_h during the PPT in the cases of surging and vibration was smaller than that in push-in, the VLT showed that the P_h in those cases was the same or higher than that in push-in. Based on the results of the cyclic triaxial CD test, the cyclic pile movement of surging or vibration during the PPT prevented soil dilation around the pile and increased P_h. When the cyclic pile movement during the PPT transformed to monotonic movement during the VLT, the soil dilation increased. Additionally, the VLT showed that the P_h in all displacement pile installation methods (i.e, push-in, surging and vibration) was higher than that of non-displacement pile (bored pile method). Therefore, it can be said that these displacement pile installation methods expand the soil around the installed pile and increase the vertical resistance.
2) The difference in horizontal pile resistance among the cases was not remarkable in the HLT in comparison with that in the VLT. Relatively high horizontal resistances were observed in the surging and push-in cases, indicating that the effect of displacement pile increased the horizontal soil resistance. Although the horizontal resistance of the pile caused by vibration was smaller than those of other cases, it was similar to that of the bored pile. The rotation centre of the pile caused by vibration was deeper than that caused by other pile installation methods. This implied that the distribution of the horizontal earth pressure on the pile shaft due to the vibration differed from those of caused by other piling methods. And, since the vertical resistance of the pile installed using vibration was higher than that of the bored pile, the effect of displacement pile to increase the soil resistance may differ between the vertical and horizontal loading direction. More studies should be performed to clarify the reason while considering the influence of the pile installation method.

REFERENCES

Bekki, H., Canou, J., Tali, B., Dupla, J. C., Bouafia, A., 2013. Evolution of local friction along a model pile shaft in a calibration chamber for a large number of loading cycles. *Comptes Rendus Mécanique* 341 (6): 499–507.

Holeyman, A. E., Legrand, C. & Rompaey, D. V. 1996. A method to predict the drivability of vibratory driven piles. *Proc. 5th International Conference on the Application of Stress-Wave Theory to Piles*: 1101–1112.

Moriyasu, S., Matsumoto, T., Aizawa, M., Kobayashi, S. & Shimono, S. 2020. Effects of cyclic behaviour during pile penetration on pile performance in model load tests. *Geotechnical Engineering Journal of the SEAGS & AGSSEA* 51(2): 150–158.

Ogawa, N., Ishihara, Y., Nishigawa, M. & Kitamura, A. 2011. Effect of surging in Press-in piling: shaft resistance and pore water pressure. *Press-in Engineering 2011, Proc. 3th IPA International Workshop in Shanghai*: 101–106.

Rodger, A.A. & Littlejohn, G. 1980. A study of vibratory driving in granular soils. *Geotechnique* 30 (3): 269–293.

Vanden Berghe, J.F. 2001. Sand strength degradation within the framework of vibratory pile driving. *Ph. D. thesis*, Universite catholique de Louvain.

White, D.J. & Deeks, A.D. 2007. Recent research into the behaviour of jacked foundation piles. *Advanced in Deep Foundations*: 3–26.

Watanabe, K. & Kusakabe, O., 2013. Reappraisal of loading rate effects on sand behaviour in view of seismic design for pile foundations. *Soils and Foundations*: 53 (2), 215–231.